Possible TeV Source Candidates In The Unidentified EGRET Sources

W. Wang*, Z.J. Jiang, C.S.J. Pun, & K.S. Cheng
Department of Physics, The University of Hong Kong, Pokfulam Road, Hong Kong, China
* the present address: Max-Planck-Institut für extraterrestrische Physik, Postfach 1312, 85741 Garching, Germany

21 March 2005

ABSTRACT
We study the γ-ray emission from the pulsar magnetosphere based on outer gap models, and the TeV radiation from pulsar wind nebulae through inverse Compton scattering using a one-zone model. We showed previously that GeV radiation from the magnetosphere of mature pulsars with ages of $\sim 10^5 - 10^6$ years old can contribute to the high latitude unidentified EGRET sources. We carry out Monte Carlo simulations of γ-ray pulsars in the Galaxy and the Gould Belt, assuming the pulsar birth rate, initial position, proper motion velocity, period, and magnetic field distribution and evolution based on observational statistics. We select from the simulation a sample of mature pulsars in the Galactic plane ($|b| \leq 5°$) and in the high latitude ($|b| > 5°$) which could be detected by EGRET. The TeV flux from the pulsar wind nebulae of our simulated sample through the inverse Compton scattering by relativistic electrons on the microwave cosmic background and synchrotron seed photons are calculated. The predicted fluxes are consistent with the present observational constraints. We suggest that strong EGRET sources can be potential TeV source candidates for present and future ground-based TeV telescopes.

Key words: radiation mechanisms: nonthermal – stars: statistics – stars: neutron – pulsars: general – γ-rays

1 INTRODUCTION

There are about 170 unidentified γ-ray sources in the third EGRET catalog, and nearly one third of these sources lie close to the Galactic plane $|b| < 5°$ (Hartman et al. 1999). Most of those unidentified sources in the Galactic plane can be identified as γ-ray pulsars, possibly Geminga-like pulsars which are radio quiet (Cheng & Zhang 1998; Zhang, Zhang & Cheng 2000). For the medium and high latitude sources, it has been suggested that some of them are associated with the supernova remnants in the nearby Gould Belt (Gehrels et al. 2000; Grenier 2000). In addition, Harding & Zhang (2001) used the polar cap model (Daugherty & Harding 1996) to investigate if γ-ray pulsars viewed at a large angle to the neutron star magnetic pole could contribute to unidentified EGRET sources in the medium latitudes associated with the Gould Belt. Their results suggest that at least some of radio-quiet Gould Belt sources detected by EGRET could be such off-beam γ-ray pulsars.

At the same time, these γ-ray pulsars could produce wind nebulae through the interactions between relativistic wind particles with the interstellar medium (ISM). The pulsar wind nebulae will contribute to the production of non-pulsed X-ray emission by synchrotron processes (Chevalier

2000), and TeV photons through inverse Compton scattering (ICS, Aharonian, Atoyan & Kifune 1997). These excessive TeV photons have been detected in some known pulsar wind nebulae, such as Crab, Vela, PSR 1706-44, possibly Geminga (Kifune et al. 1995; Yoshikoshi et al. 1997; Aharonian et al. 1999; Lessard et al. 2000). Therefore, if γ-ray pulsars contribute to the unidentified EGRET sources, it is expected that possible TeV signals could be detected in these EGRET sources. Several groups have searched for TeV signals in the error boxes of unidentified EGRET sources, for example, with the HEGRA AIROBICC array (Aharonian et al. 2002a), and the Whipple 10m Gamma-Ray Telescope. No TeV source detection has been confirmed at the Whipple, with only an upper limit TeV flux of about 20 EGRET sources determined at $\sim (3-6) \times 10^{-11}$ photon cm^{-2} s^{-1} (Fegan & Weekes 2004). Deep observations of the Cygnus region using HEGRA (Aharonian et al. 2002b) showed that an unidentified TeV source in the vicinity of Cygnus OB2 with an integral flux $F(> 1 \text{ TeV}) \sim 5 \times 10^{-13}$ photon cm^{-2} s^{-1}, at the edge of the 95% error circle of the EGRET source 3EG J2033+4188. However, no connection between the EGRET source and TeV signal has yet been confirmed.

It has been shown that GeV photons can be produced in the pulsar magnetosphere in outer gap models (Cheng et

al. 1986; Zhang & Cheng 1997). A revised outer gap model (Zhang et al. 2004) take into account the effect of the inclination angle α between the magnetic axis and the rotational axis, which can determine the gap size of the outer gap. This allows some pulsars with appropriate combinations of α, P, and B, to maintain the outer gap for at least $\sim 10^6$ years. Their advanced ages allow these pulsars enough time to move up to high Galactic latitude as weak γ-ray sources. This leads Cheng et al. (2004a) to propose that mature γ-ray pulsars with ages $\sim 10^5 - 10^6$ years old can contribute to the unidentified EGRET sources. These mature pulsars also remain active to produce relativistic wind particles, and form compact wind nebulae. In addition, TeV photons can be created in the nebulae through the ICS process. In this paper, we study the possible connection between TeV γ-ray sources and the Unidentified EGRET sources. Since we do not know if the Unidentified EGRET sources are pulsars, even if they are pulsars and we still do not know their properties, i.e. period, magnetic field, inclination angle, distance etc. Without these parameters we cannot calculate their γ-ray properties. Therefore, we apply a statistical approach by Monte Carlo simulation to study the Unidentified Gamma-ray EGRET Sources. First we will simulate the galactic pulsar population and use the outer gap model to calculate the MeV-GeV photon power from these simulated pulsars. We have ignored the contribution from the polar gap for simplicity. We can determine which simulated pulsars can be detected by EGRET in γ-rays, we call them γ-ray loud pulsars. The next step is to calculate the γ-ray emission from pulsar wind based on the simulated pulsar parameters. We should point out that the distribution of γ-ray loud pulsars are model dependent. Subsequently we study the TeV γ-ray emitted from the pulsar wind when they interact with their ambient interstellar medium. We argue that strong EGRET sources may be potential TeV source candidates for current and future TeV telescopes.

In §2, theories of radiation of mature pulsars from both inside and outside the light cylinder will be briefly reviewed. Detailed discussions of the ICS processes of relativistic electrons on the background and synchrotron photons using a one-zone wind nebula model (Chevalier 2000; Cheng, Taam & Wang 2004b) will be presented in § 3. In § 4, the properties of the identified TeV pulsar wind nebulae sources are reviewed and compared with our models. In § 5, we describe the Monte Carlo simulations, similar that carried in Cheng et al. (2004a), for deriving the distribution of γ-ray pulsars in the Galaxy and Gould Belt which can be detected by EGRET. We then calculate the expected GeV and TeV fluxes from these γ-ray pulsars generated by the Monte Carlo simulations. The TeV flux distribution of the unidentified EGRET source candidates, which could possibly be detected by the present and future ground-based TeV telescopes, will be presented in § 6. Finally, we present our summary and discussions in § 7.

2   RADIATION THEORIES ASSOCIATED WITH PULSARS

In this section, we will review the emission properties of mature pulsars whose ages are from $\sim 10^5 - 10^6$ years old. The high energy radiation of mature pulsars can come both from the pulsar magnetosphere inside light cylinder, and from the pulsar wind nebulae outside light cylinder.

2.1   Inside light cylinder - outer gap model

We present the γ-ray emission properties of pulsars using the outer gap models originally proposed by Cheng et al. (1986a,b). Based on the model, Zhang & Cheng (1997) have developed a self-consistent mechanism to describe the high energy radiation from spin-powered pulsars. In the model, relativistic charged particles from a thick outer magnetospheric accelerator (outer gap) radiate through the synchro-curvature radiation mechanism (Cheng & Zhang 1996) rather than the synchrotron and curvature mechanisms in general, producing non-thermal photons from the primary $e^\pm$ pairs along the curved magnetic field lines in the outer gap.

The characteristic emission energy of high energy photons emitted from the outer gap is given by (Zhang & Cheng 1997)

$$E_{\gamma,c} \simeq 5 \times 10^7 f^{3/2} B_{12}^{3/4} P^{-7/4} \left(\frac{r}{R_L}\right)^{-13/8} \text{eV}, \qquad (1)$$

where P is the rotation period, B_{12} is the dipolar magnetic field in units of 10^{12} G, $R_L = cP/2\pi$ is the light cylinder radius, r is the distance to the neutron star, and f is the fractional size of the outer gap. The γ-ray spectrum drops exponentially beyond the energy $E_{\gamma,c}$.

The factor f, defined as the the ratio between the mean vertical separation of the outer gap boundaries in the plane of the rotation axis and the magnetic axis to the light cylinder radius, is limited by the pair production between the soft thermal X-rays from the neutron star surface and the high energy γ-ray photons emitted from the outer gap region, and can be approximated as $f \simeq 5.5 P^{26/21} B_{12}^{-4/7}$. The size of f in turn determines the total γ-ray luminosity of the pulsar which is given by (Zhang & Cheng 1997)

$$L_\gamma \simeq f^3 L_{\text{sd}}, \qquad (2)$$

where $L_{\text{sd}} = 3.8 \times 10^{31} B_{12}^2 P^{-4}$ erg s^{-1} is the pulsar spin down power. However, the estimation of gap size f by Zhang & Cheng (1997) does not include the effect of inclination angle and their model can produce very few pulsars with age $\sim 10^5 - 10^6$ yrs old. Zhang et al. (2004) have studied the properties of outer gap by including the effect inclination angle. Also instead of taking half of the light cylinder as the representation of the outer gap, they have calculated the average outer gap size and use it as the representation of outer gap. This is very important for statistical study. Cheng et al (2004a) show that in Monte Carlo simulation even if the inclination angle of pulsars is randomly selected from a uniform distribution, the simulated γ-ray pulsars detected by EGRET in the galactic plane are younger and tend to have larger inclination angle. On the other hand, γ-ray pulsars detected by EGRET in higher latitude are older and have a smaller inclination angle. In other words, even if the seed distribution has a uniform distribution, a non-uniform distribution can be generated by the γ-ray selection effects. In this paper, we intend to use Monte Carlo method to study GeV and TeV γ-ray properties of pulsars so we adopt the model of Zhang et al. (2004) to determine the size of the outer gap. Assuming that the representative

region of the outer gap is the average distance to the gap, the mean fractional size of the outer gap can be approximated as $f(\alpha, P, B) \approx \eta(\alpha, P, B)f(P, B)$, where $\eta(\alpha, P, B)$ is a monotonically increasing function of α, B, and P. The value of η roughly decreases by a factor 3 from large inclination angles to smaller angles (Zhang et al. 2004). These γ-rays from the pulsar magnetosphere will contribute to the pulsed GeV photons in γ-ray pulsars detected by EGRET.

In general the differential energy spectrum of γ-ray flux for each pulsar is different. In principle we can calculate it if the pulsar parameters are specified. However, it is very difficult to do in a Monte Carlo simulation, in which we need to deal with over ten million pulsars. EGRET has detected six γ-ray pulsars and their energy spectra from 100 MeV to a few GeV are all very close to E_γ^{-1} (Hartman et al. 1999). For thin outer gap pulsars, it has been shown that the energy spectrum is proportional to $E_\gamma^{-1}log(E_{max}/E_\gamma) \propto E_\gamma^{-1}$ (Cheng, Ho and Ruderman 1986b; Cheng and Ding 1994). For simplicity in the Monte Carlo simulation, we will approximate the expected energy differential γ-ray flux of the pulsar as

$$F(E_\gamma) \simeq \frac{L_\gamma}{\Delta\Omega d^2 E_\gamma}, \qquad (3)$$

where d is the distance of the pulsar, and $\Delta\Omega$ is the the solid angle of γ-ray beaming. The value of $\Delta\Omega$ generally varies with different pulsars. For simplicity, we assume a constant beaming solid angle $\Delta\Omega \sim 1$ sr in all our analyses. In order to compare our model results with observations, we calculate the expected integral EGRET flux of our model γ-ray pulsars using the formula

$$S_\gamma(E_\gamma \geq 100\text{MeV}) = \int_{100\text{MeV}}^{E_{max}} F(E_\gamma)dE_\gamma, \qquad (4)$$

where E_{max} is the maximum γ-ray energy detected by EGRET, chosen to be 50 GeV.

Here, we have ignored the γ-ray contribution from polar cap, which could be important for Unidentified EGRET Sources (Gonthier et al. 2002). However, the phase-resolved EGRET data of the Crab pulsar (Cheng , Ruderman and Zhang 2000), Geminga (Zhang and Cheng 2001) and the Vela pulsar (Romani 1996)can be explained very well by outer gap model and it appears that polar cap emission seems unimportant. Most Recently, Muslimov & Harding(2004) have suggested that the slot gap model could be able to explain the phase-resolved data as well. Since the distributions of simulated γ-ray pulsars are model dependent, in this paper we will ignore the contribution of γ-ray from the polar cap for simplicity.

2.2 Outside light cylinder - pulsar wind nebulae

Previous models on the pulsar wind nebula (e.g., Kennel & Coroniti 1984; Chevalier 2000) mainly concentrate on the bright nebulae produced by interactions between young pulsar wind particles and the supernova remnant (SNR). On the other hand, while there are no SNR surrounding the mature pulsars, they remain active enough to produce the relatively faint, compact synchrotron nebulae through interactions between the relativistic wind particles and interstellar medium. In this work, we use the one-zone model to describe high energy radiation from pulsar wind nebulae (Chevalier 2000).

In the model, the relativistic electrons in the shock waves emit X-rays through synchrotron radiation. This model can well explain the X-ray luminosity and spectral properties of pulsar wind nebulae (Cheng et al. 2004b).

Mature pulsars move at a high proper velocity after their birth, and can form bow shock structure to produce synchrotron wind nebulae when the pulsar proper motion velocity is larger than the sound speed of the ambient interstellar medium (ISM). The characteristic size of the shock wave produced by interactions between the pulsar wind particles and the ISM is referred to as the termination radius, R_s, and can be derived from

$$R_s = (L_{sd}/2\pi\rho v_p^2 c)^{1/2} \sim 10^{16} L_{sd,34}^{1/2} n^{-1/2} v_{p,350}^{-1} \text{ cm}, \qquad (5)$$

where $\rho = nm_p$, $n = 1$ cm^{-3} is the number density of ISM, m_p is the proton rest mass, v_p is the pulsar velocity in units of 350 km s^{-1} (cf. § 5.2), and $L_{sd,34}$ is the spin down power of the pulsar in units of 10^{34} erg s^{-1}.

We have assumed the pulsar wind can carry away most of pulsar spin-down power (L_{sd}) and deposit in the shock waves when the wind interacts with the interstellar medium. In general, the energy in the shock waves is stored in the magnetic field, the energetic protons (ions) and electrons. However, the fractional energy density of the magnetic field ϵ_B is low (typically, $\epsilon_B \sim 0.001 - 0.01$, Kennel & Coroniti 1984), then by assuming equipartition energy between protons and electrons, we obtain $\epsilon_p \sim \epsilon_e \sim 0.5$. For a given ϵ_B, the magnetic field at the termination radius is estimated as $B = (6\epsilon_B L_{sd}/R_s^2 c)^{1/2}$. At the shock front, the electron energy distribution is $N(\gamma) \propto \gamma^{-p}$ for $\gamma_m < \gamma < \gamma_{max}$, where $\gamma_m = [(p-2)/(p-1)]\epsilon_e\gamma_w$, and γ_w is the Lorentz factor of the pulsar wind particles.

We derive the value of γ_{max} with two methods. First, an estimate for γ_{max} can be obtained by equating the synchrotron cooling timescale to the electron acceleration timescale. The former timescale is given by $t_{syn} = 6\pi m_e c/\sigma_T\gamma B^2$, and the latter timescale is given by $t_{acc} = \gamma m_e c/eB$, leading to $\gamma_{max,1} = (6\pi e/\sigma_T B)^{1/2} \sim 10^{10}B_{-5}^{-1/2}$, where σ_T is the Thompson cross section, and B_{-5} denotes $B/10^{-5}$G. Second, we can estimate γ_{max} by equating the acceleration timescale and diffuse timescale of electrons. The electron diffuse time in the termination radius can be estimated as $t_{diff} \sim (R_s/r_L)^2 r_L/c$, where $r_L \sim \gamma m_e c^2/eB$ is the Larmor radius. This gives a maximum Lorentz factor of $\gamma_{max,2} \sim 10^8 B_{-5}R_{s,16}$, where $R_{s,16} = R_s/10^{16}$ cm. We will assume

$$\gamma_{max} = \min(\gamma_{max,1}, \gamma_{max,2}) \qquad (6)$$

in the following discussion.

The Lorentz factor of wind particles cannot be too small for the production of the synchrotron nebulae, requiring for example $\gamma_w > 10^4$. Theoretical constraints on γ_w are still difficult to determine at present. In this paper, we use of the arguments of Ruderman (1981) and Arons (1983) that large fluxes of protons (ions) can be extracted from neutron stars and can be accelerated in the parallel electric field in the magnetosphere. We also assume that the initial Poynting flux can be converted into particle thermal and kinetic energy well within the termination radius, and that the Lorentz factors of electrons and protons are the same. For young pulsars like the Crab pulsar and the Vela pulsar, a large number of electron and positron can be produced in the

outer magnetosphere (Cheng, Ruderman & Ho 1986b) and hence electrons/positrons are main energy carriers in the pulsar wind. However, for mature pulsars with age $> 10^5$ years old. The outer gap cannot produce too many pairs (Zhang & Cheng 1997). The pair creation will be mainly in polar cap, however, the ratio between electron number and proton number is $\leq m_p/m_e$, in particular for the space-charge-limited flow situation (Arons & Scharlemann 1979; Cheng & Ruderman 1980). Since we will show that the main contributors of TeV γ-ray sources are mature pulsars, so we shall assume that protons are main energy carriers of pulsar wind. We want to point out that this assumption does not conflict with the equipartition assumption in the shock waves because pulsar wind energy will be redistribute when the wind interacts with the interstellar medium in the shock waves.

The protons can then carry away most of spin down power in this scenario (Coroniti 1990). Thus, we can derive the spin down power as $L_{\rm sd} \sim \dot{N}\gamma_w m_p c^2$, where $\dot{N}$ is the outflow current from the surface. This outflow current should be of the same order as the Goldreich-Julian current (Goldreich & Julian 1969) which is given as $\dot{N} \simeq 1.35 \times 10^{30} B_{12} P^{-2}$ s^{-1} $\propto L_{\rm sd}^{1/2}$. For mature pulsars with $L_{\rm sd} \sim 10^{34-36}$ erg s^{-1}, we derive a typical value of $\gamma_w \sim 10^6$.

The critical synchrotron frequency of relativistic electrons with a Lorentz factor γ is $\nu(\gamma) = \gamma^2 eB/2\pi m_e c$. The synchrotron radiation properties from the pulsar wind nebulae depend on two characteristic frequencies: ν_m, radiated by the electrons with the Lorentz factor of γ_m, and the cooling frequency, ν_c, given as $\nu_c = e/(2\pi m_e cB^3)[(6\pi m_e c)/(\sigma_T t_0)]^2$, where t_0 is the characteristic timescale of the nebula estimated from the flow timescale in a characteristic radiation region. If we define a characteristic time scale $t_0 \sim R_s/v_p \sim 10^9$ s, and $B \sim 10^{-5}$ G, then the cooling frequency $\nu_c \sim 10^{19}$ Hz. This corresponds to a characteristic cooling Lorentz factor $\gamma_c \sim 10^9$, which is significantly larger than γ_m. Therefore, we can derive the luminosity and spectral properties of synchrotron radiation from the pulsar wind nebulae. When $\nu_m < \nu < \nu_c$, it can be described as a non-thermal spectrum with a power law photon index $\Gamma \sim (p+1)/2$, and a synchrotron radiation luminosity is estimated by (also see Chevalier 2000; Cheng et al. 2004b)

$$L_{\rm syn}(\nu) \simeq \frac{\sigma_T e^{(p-3)/2}(nm_p)^{(p+1)/4}}{9m_e^{(p-1)/2}c^{(p-1)/2}}\epsilon_e^{p-1}\epsilon_B^{(p+1)/4}$$
$$v_p^{(p+1)/2}\gamma_w^{p-2}t_0 L_{\rm sd}\nu^{(3-p)/2}. \qquad (7)$$

This case is called slow cooling regime. On the other hand in the fast cooling regime when $\nu > \nu_c$, the emission spectrum will steepen because of the cooling of relativistic electrons, the photon index $\Gamma \sim (p+2)/2$, and the luminosity is

$$L_{\rm syn}(\nu) \simeq \frac{1}{2}(\frac{p-2}{p-1})^{p-1}(\frac{e}{m_e c})^{(p-2)/2}(nm_p)^{(p-2)/4}\epsilon_e^{p-1}$$
$$\epsilon_B^{(p-2)/4}\gamma_w^{p-2}v_p^{(p-2)/2}L_{\rm sd}\nu^{(2-p)/2}. \qquad (8)$$

3   TEV PHOTONS FROM PULSAR WIND NEBULAE THROUGH INVERSE COMPTON PROCESSES

The synchrotron radiation of relativistic electrons in the pulsar wind nebulae can well contribute to non-thermal radio to X-ray emissions. At the same time, the inverse Compton scattering (ICS) of the same relativistic electrons on the ambient photon fields results in the production of the very high energy TeV photons observed (de Jager & Harding 1992; Atoyan & Aharonian 1996; Aharonian, Atoyan & Kifune 1997). In this section, we will discuss two cases of the ICS processes of two different types of seed photons, namely, background and synchrotron photons. We can see that the Inverse Compton luminosity is sensitively dependent on the properties of the seed photons.

3.1   Inverse Compton Scattering from background photons

The relative magnitude between the emission from synchrotron and ICS processes depend on the magnetic field B and the photon field density $w_{\rm ph}$. The magnetic field in the interstellar medium is typically within the range $(0.3-1) \times 10^{-5}$ G. Synchrotron X-ray photons and γ-ray photons from ICS have been shown to be produced in regions of different magnetic fields (Aharonian et al. 1997). In this paper, we assume for simplicity that the X-rays and γ-rays come from the same region with a magnetic field $B \sim 10^{-5}$ G.

The photon energy density surrounding the pulsars can be attributed to several origins: first, the cosmic microwave background (CMB) radiation contributes a constant energy density $w_{\rm CMB} \sim 4 \times 10^{-13}$erg cm^{-3}, second, the diffuse galactic dust far-infrared (FIR) and star light near-infrared and optical background (sl), and third, possible radiation field of local origin. The density of the galactic background field varies from site to site, with an average values $w_{\rm FIR} \sim 10^{-13}$ erg cm^{-3} and $w_{\rm sl} \sim 10^{-12}$ erg cm^{-3} (Mathis, Metzger & Panagia 1983). Although the energy density of the galactic radiation background is higher than that of the CMB, its importance is strongly reduced in the energy region above 100 GeV due to the Klein-Nishina effect (Aharonian et al. 1997). Therefore we consider here only the CMB photon field as the external seed photons for the production of TeV photons.

The characteristic energy, $E_{\rm syn}$, of synchrotron radiation from relativistic electrons with typical Lorentz factor γ is given as

$$E_{\rm syn} = h\nu_{\rm syn} = \hbar\gamma^2 eB/m_e c \sim 1B_{-5}(\gamma/10^8)^2 \text{ keV}. \qquad (9)$$

The characteristic energy of the photons from the ICS of these same energy electrons on the CMB photons is given by

$$E_{\rm IC} = \gamma^2 h\nu_0 \sim 1(\gamma/10^8)^2(h\nu_0/\varepsilon_{\rm CMB}) \text{ TeV}, \qquad (10)$$

where $\varepsilon_{\rm CMB} \sim 10^{-4}$ eV is the energy of the CMB photons. The ratio of the luminosity of the emission from the ICS process to that from synchrotron radiation can be simply obtained as ($\gamma h\nu_0 < m_e c^2$)

$$\frac{L_{\rm IC}}{L_{\rm syn}} = \frac{w_{\rm CMB}}{w_B}, \qquad (11)$$

where $w_B = B^2/8\pi$ is the energy density of magnetic field. To derive the γ-ray luminosity of TeV photons by the ICS process, we can first estimate the synchrotron X-ray luminosity of the pulsar wind nebulae using the one-zone model discussed in § 2.2.

The TeV photon luminosity and flux distributions will be studied in detail in § 6 using a simulated sample of mature pulsars. Here, we use some typical pulsar parameters for a simple estimate. According to equations (9) and (10), TeV photons through ICS produced by relativistic electrons correspond to X-rays (~ 1 keV) through synchrotron processes. In the calculation, $\nu \sim 10^{18}$ Hz denotes the X-rays through the synchrotron process, and we take some typical parameters of pulsars and nebulae to find the TeV luminosity: $L_{\rm sd} \sim 10^{34}$ erg s^{-1}, $\epsilon_e \sim 0.5$, $\epsilon_B \sim 0.01$, $\gamma_w \sim 10^6$, $R_s \sim 10^{16}$ cm, the electron energy spectral index $p = 2.2$, then we obtain the TeV luminosity by ICS processes $L_{\rm IC}({\rm TeV}) \sim 10^{31}$ erg s^{-1}.

The spectral profile is also related to the synchrotron process. As discussed in §2.2, there exist three Lorentz factors of the relativistic electrons γ_m, γ_{max}, and γ_c. The Lorentz factor of the ICS electrons should satisfy $\gamma h\nu_{\rm CMB} < m_e c^2$, which gives a critical Lorentz factor $\gamma_{cut} \sim 10^9$. Then when the Lorentz factors satisfy the relation $\gamma_m < \gamma_c < \gamma_{cut} \leq \gamma_{max}$, for ICS electrons with γ between γ_m and γ_c, the ICS spectrum will show a power-law with a photon index $\Gamma = (p+1)/2$, for γ between γ_c and γ_{cut}, the photon index becomes $\Gamma = (p+2)/2$. For ICS electron γ above γ_{cut} or γ_{max}, the spectrum will become an exponential decay form reflecting a high energy cut-off. For mature pulsars discussed above with $\gamma_{max} \sim 10^8$, a cut-off energy at $\sim$1 TeV will be produced.

3.2 Synchrotron self-Compton scattering contribution

Using the synchrotron spectrum as the sources of seed photons, we can compute the resulting ICS emission (called synchrotron self-Compton, SSC, photons). Similar to the original synchrotron spectrum, the up-scattered component also consists of two characteristic energies, $E_m^{\rm SSC} \sim h\gamma_m^2 \nu_m$, and $E_c^{\rm SSC} \sim h\gamma_c^2 \nu_c$. In addition, the condition $\gamma h\nu(\gamma) < m_e c^2$ will give a characteristic critical factor $\gamma_{\rm crit} \sim 2 \times 10^6$ for $B = 10^{-5}$ G and a critical energy $E_{\rm crit} \sim \gamma_{\rm crit} m_e c^2$. Due to the limitation that $\gamma_{max} h\nu_0 < m_e c^2$, we can find a frequency ν_0 such that if $\nu_0 > \nu_m$, $E_{cut}^{\rm SSC} \sim \gamma_{max} m_e c^2 \sim 50(\gamma_{max}/10^8)$ TeV. In case of $\nu_0 < \nu_m$, a lower limit of $\gamma'_m h\nu_m \sim m_e c^2$ is required, thus implying a cut-off energy $E_{cut}^{\rm SSC} \sim \gamma'_m m_e c^2 \sim 10$ TeV for $B \sim 10^{-5}$ G and $\gamma_m \sim 10^5$. If $E_m^{\rm SSC} < E_c^{\rm SSC} < E_{cut}^{\rm SSC}$, then the SSC spectrum will show a power-law with a photon index $\Gamma = (p+1)/2$. for photon energy below $E_c^{\rm SSC}$, and an index $\Gamma = (p+2)/2$ for photon energy above $E_c^{\rm SSC}$. For photon energy $> E \sim \gamma_{crit} m_e c^2$, the energy spectrum of SSC becomes steeper because of the Klein-Nishina effect (Aharonian et al. 1997).

In general, the intensity of the ICS emission relative to the synchrotron radiation can be estimated by considering the ratio of the energy density of synchrotron radiation and the magnetic field, $w_{\rm syn}/w_B$. In our one-zone model, synchrotron radiation comes from the termination radius R_s. We approximate the synchrotron energy density as $w_{\rm syn} \sim 3L_{\rm syn}t_f/4\pi R_s^3$, where $t_f \sim R_s/c$. The SSC pho-

ton energy is given by $E_{\rm SSC} \sim \gamma^2 h\nu$, where $\nu \sim \gamma^2 eB/m_e c$. Because the relativistic electrons producing the TeV photons by SSC correspond to a characteristic Lorentz factor $\gamma \sim 10^6 < \gamma_c$ (assuming $B \sim 10^{-5}$ G and $t_0 \sim 10^9$ s), we should apply equation (7) to compute the energy density and luminosity of low energy synchrotron seed photons. The ratio of the SSC and synchrotron luminosities can be given by

$$\frac{L_{\rm SSC}}{L_{\rm syn}} \simeq \frac{\sigma_T e^{(p-3)/2}(nm_p)^{(p+1)/4}}{9m_e^{(p-1)/2}c^{(p-1)/2}} \epsilon_e^{p-1}\epsilon_B^{(p-3)/4}$$
$$v_p^{(p+1)/2}\gamma_w^{p-2}t_0\nu_{\rm seed}^{(3-p)/2}. \qquad (12)$$

Assuming $\nu_{\rm seed} \sim 10^{14}$ Hz, $t_0 \sim 10^9$ s, and taking the other parameters the same as those in § 3.1, we determine the luminosity of TeV photons produced by SSC is about $L_{\rm SSC}({\rm TeV}) \sim 10^{30}$ erg s^{-1}.

4 IDENTIFIED TEV SOURCES OF PULSAR WIND NEBULAE

The present TeV telescopes have detected excessive TeV photons from three γ-ray pulsars, namely, Crab, Vela and PSR 1706-44, with a possible detection from Geminga (see reviews by Aharonian 1999; Weekes 2004). Their γ-ray emissions in the GeV band are dominated by contributions from the pulsar magnetosphere, as predicted in the outer gap model (§ 2.1). However, no pulsed TeV photons are detected by the present telescopes (Kifune et al. 1995; Yoshikoshi et al. 1997; Aharonian et al. 1999; Lessard et al. 2000), thus implying that the TeV photons mainly come from their wind nebulae. In this section, we check our one-zone model by estimating the TeV signals from these four sources. Because of the simplified nature of these models, we do not expect the reproduce the detailed properties of the nebula. More detailed discussions for individual sources have been addressed by other authors (e.g. de Jager & Harding 1992; Atoyan & Aharonian 1996; Aharonian, Atoyan & Kifune 1997).

4.1 Crab nebula

The Crab nebula is the first pulsar wind nebulae with TeV signal detection (Weekes et al. 1989), and it has been extensively studied by many TeV detectors since, for example, Milagro (Atkins et al. 2003), HEGRA (Aharonian et al. 2000), Whipple (Lessard et al. 2000), Tibet (Amenomori et al. 1999), and CANGAROO (Tamimori et al. 1998). Detailed spectral and flux information have been obtained. The Crab TeV spectrum can be fitted in the energy range above 1 TeV by a simple power law with a photon index $\sim 2.5\pm0.2$, and show no cut-off up to 100 TeV. The TeV luminosity is estimated to be $\sim 10^{34}$ erg s^{-1}.

Atoyan & Aharonian (1996) discussed the radiation mechanism of the Crab nebulae based on the model of Kennel & Coroniti (1984), and fit the observed data from radio to GeV by synchrotron radiation, and the TeV band through ICS processes. With a complicated spatial structure, the Crab nebula probably cannot be fully described in our one-zone model. What we present in the following should therefore be treated as a rough check.

The magnetic field in the Crab nebula is relatively high

at $B \sim 10^{-3} - 10^{-4}$ G (Hester et al. 1996), which significantly reduces the relative contributions from the ICS processes. With a ratio $w_{CMB}/w_B \leq 10^{-4}$, the SSC contribution to TeV photons should be the dominated component. Assuming $B \sim 10^{-4}$ G, we derive the cooling Lorentz factor of electrons to be $\gamma_c \sim 10^6$, and the characteristic timescale $t_0 \sim 3 \times 10^{10}$ s. The implied cooling energy $E_c^{SSC} \sim 1$ TeV, which is only 1% of the predicted SSC cut-off. Therefore, above 1 TeV, the photon index of the ICS spectrum is given by $\Gamma = (p+2)/2$, where $p > 2$. On the other hand, the observed TeV spectrum of the Crab nebula implies that $p \sim 3$. However, from the observed synchrotron X-ray spectrum of the Crab nebula (Willingale et al. 2001), $\Gamma = (p+2)/2 \sim 2.1$, which gives $p \sim 2.2$. Since $\gamma_{crit} \sim \gamma_c \sim 10^6$ in the Crab nebula, and above $\gamma_{crit} m_e c^2 \sim 1$ TeV, the SSC spectrum can be steeper than $(p+2)/2$, hence agreeing with the observations. The discrepancy may also result from the spatial variations of the electron spectrum and magnetic field in the Crab nebula considered by other models (de Jager & Harding 1992; Atoyan & Aharonian 1996; Sollerman et al. 2000), which are not considered in our one-zone model.

Despite the Crab nebula has a very large size, the TeV photons come from the central region ~ 1 pc (Atkins et al. 2003). The termination radius of the nebula is about $R_s = 4 \times 10^{17}$ cm. In our one-zone model, we can take $\epsilon_e \sim \epsilon_B \sim 0.5$, $p = 2.2$, and $\gamma_w \sim 10^7$, to estimate the synchrotron luminosity and energy density. At $\nu \sim 10^{14}$ Hz, the luminosity $L_{syn} \sim 10^{36}$ erg s^{-1} and $w_{syn}/w_B \sim 0.03$. Therefore the SSC contribution to TeV luminosity is $L_{SSC} \sim 3 \times 10^{34}$ erg s^{-1}, which is comparable with the observed value.

4.2   Vela and PSR 1706-44

Yoshikoshi et al. (1997) used the 3.8 m imaging Cerenkov telescope near Woomera, South Australia to detect the TeV photons of the Vela pulsar region. The detected TeV γ-ray flux is 2.9×10^{-12} photon cm^{-2} s^{-1}, corresponding to a luminosity of 3×10^{32} erg s^{-1} assuming the distance of Vela to be 300 pc. Similar to Vela, PSR 1706-44 has also be detected in the TeV energy range (Kifune et al. 1995; Chadwick et al. 1998). The flux above a threshold of 1 TeV is $\sim 10^{-11}$ photon cm^{-2} s^{-1}. **However, recent observations of HESS reported non-detection of PSR 1706-44, with an upper limit flux $\sim 1.3 \times 10^{-12}$ erg cm^{-2} s^{-1} (Aharonian et al. 2005). The reason of the observational discrepancy is unknown, possibly the TeV emission could be variable on a time scale of years, e.g. in the different medium environments. Assuming a distance of 1.5 kpc, the TeV luminosity is lower than 4×10^{32} erg s^{-1}.** TeV spectral information has been obtained for neither of the two sources.

Vela and PSR 1706-44 have the nearly same spin down power of a few times 10^{36} erg s^{-1}. This suggests that their nebulae have similar properties moving in the interstellar medium. Assuming $\epsilon_e \sim 0.5$ and $\epsilon_B \sim 0.001$, we estimate the magnetic field B in the two pulsar wind nebulae. According to the Chandra observation of Vela (Pavlov et al. 2001), together with $R_s \sim 10^{17}$ cm (Cheng et al. 2004b), and $L_{sd} \sim 6.9 \times 10^{36}$ erg s^{-1}, we estimate that $B \sim 10^{-5}$ G. For PSR 1706-44, using $L_{sd} \sim 3.4 \times 10^{36}$ erg s^{-1}, and $R_s \sim 3 \times 10^{17}$ cm (Finley et al. 1998; Cheng et al. 2004b),

we estimate $B \sim 3 \times 10^{-6}$ G. The observed nebula photon indices of Vela and PSR 1706-44 in X-rays is about 1.7, which required $\nu_c > \nu_x$, and $p \sim 2.4$. As discussed in § 3.2, the ICS processes by CMB photons would be the dominating contributor of TeV flux of the two pulsar wind nebulae. The proper motion velocity of Vela is about 65 km s^{-1} (Pavlov et al. 2001). Assuming for the two pulsars $t_0 \sim 10^{10}$ s, $\gamma_w \sim 10^6$, and $\nu \sim 3 \times 10^{17}$ Hz, to find the synchrotron radiation, we estimate the TeV luminosities of the pulsar nebulae to be $\sim 5 \times 10^{32}$ erg s^{-1} for Vela, and $\sim 2 \times 10^{33}$ erg s^{-1} for PSR 1706-44. **So the assumption of standard model parameters may predict the higher luminosities than the observations.**

4.3   Geminga

Geminga is a strong γ-ray pulsar source in the GeV energy range, but is very weak in other energy band. For example, its X-ray luminosity (including pulsar and the wind nebula) is about $\sim 10^{30}$ erg s^{-1} (Caraveo et al. 2003). Observations of Geminga have not been yielded significant excess of TeV signals. Aharonian et al. (1999) obtained an upper limit which is only $\sim 13\%$ of that the Crab nebula, corresponding to a luminosity of $< 6 \times 10^{30}$ erg s^{-1} assuming a distance of 160 pc.

The wind nebula around Geminga has a typical bow shock structure, with a non-thermal X-ray spectrum and a photon index $\Gamma \sim 1.6$, which corresponds to $p \sim 2.2$ (Caraveo et al. 2003). Assuming that the Geminga pulsar moves in the interstellar medium of density $n \sim 1$ cm^{-3} with a proper motion velocity of $v_p \sim 120$ km s^{-1} (Bignami & Caraveo 1993), and a spin down power of $L_{sd} \simeq 3.2 \times 10^{34}$ erg s^{-1}, the termination shock radius of the pulsar wind nebula can be determined as $R_s \sim 4 \times 10^{16}$ cm, with $t_0 \sim 3 \times 10^6$ s. Taking $\gamma_w \sim 10^6$, $\epsilon_e \sim 0.5$, $\epsilon_B \sim 0.01$, and $B \sim 10^{-5}$ G, Cheng et al. (2004b) explained the X-ray features of Geminga with a one-zone model. The SSC contribution to TeV flux of Geminga is also very small. The total ICS luminosity of the nebula in the TeV energy range is estimated as $\sim 3 \times 10^{29}$ erg s^{-1}, which is lower than the upper limit inferred by observations.

5   SIMULATION OF γ-RAY PULSARS IN THE GALAXY

In this section we briefly describe the Monte Carlo method, which is used to simulate the properties of the luminosity, spatial evolution, and distributions of γ-ray pulsars in the Galaxy. The detailed Monte Carlo steps can be found in Cheng & Zhang 1998; Zhang et al. 2000; Fan et al. 2001).

5.1   Monte Carlo simulation of γ-ray pulsars in the Galaxy

The basic assumptions of our Monte Carlo simulation are given as follows:

1. The birth rate of pulsar in the Galaxy is not clear, it is about one pulsar for every 50-200 years. Here we use the pulsar birth rate in the Galaxy is one pulsar per century. The age of the Gould Belt is ~ 30 yrs. Again the birth rate of pulsar in Gould Belt is not certain but a rate of 20 Myr^{-1} is

generally used (Grenier 2000). Basically the birth rates will only affect the final number of γ-ray pulsars but not their distributions.

2. The Sun is inside the Gould Belt and is located about 200 pc towards $l = 130°$ (Guillout et al. 1998). The Gould Belt has an ellipsoidal shaped ring with semi-major and minor axes equal to 500 pc and 340 pc respectively.

3. The initial position for each pulsar in the Galaxy is distributed according to the mass distribution of the Galaxy. We use the mass distribution suggested by Paczynski (1990) and Sturner & Dermer (1996). But the initial position of each pulsar is assumed to be born uniformly inside the Gould Belt.

4. The initial magnetic field $\log B$ is assumed to be Gaussian, with a mean value of 12.5 and a dispersion of 0.3. Since the pulsars in our simulation sample are all younger than 10 million years, and the magnetic field does not decay in 10 Myr (Bhattacharya et al. 1992), we have ignored the field decay for these pulsars.

5. The initial period is chosen to be $P_0 = 10$ ms, and the period at time t is given by $P(t) = (P_0 + 1.95 \times 10^{-39} B^2 t)^{1/2}$.

6. The initial velocity of each pulsar is the vector sum of the circular rotation velocity at the birth location and the random velocity from the supernova explosion (Paczynski 1990). The circular velocity is determined by the Galactic gravitational potential and the Maxwellian three-dimensional root-mean-square (rms) velocity is assumed to be $\sqrt{3} \times 100$ km s^{-1} (Lorimer et al. 1997). Furthermore, the pulsar position at time t is determined following its motion in the Galactic gravitational potential. Using the equations given by Paczynski (1990) for the given initial velocity, orbit integrations are performed using the fourth-order Runge Kutta method with variable time steps on the variables R, V_R, z, and V_z. The sky positions and distances to the simulated pulsars can then be calculated.

7. The inclination angle α of each pulsar is chosen randomly from a uniform distribution (Biggs 1990).

8. The γ-ray background is non-uniform over the sky, therefore the γ-ray threshold varies over the sky as well. In general the threshold will be higher in the galactic plane and lower higher latitude. It is generally accepted that a detectable sources should be at least to have a signal 5σ above the background, which is roughly equivalent to the likelihood criterion $\sqrt{TS} \geq 5$(Hartman et al. 1999). Recently, Gonthier et al. (2002) have estimated that photon flux thresholds for EGRET are 1.6×10^{-7}cm^{-2} s^{-1} for sources located in $|b| < 10°$ and 7×10^{-8}cm^{-2} s^{-1} for sources located in $|b| > 10°$ respectively. In our simulation, we use energy flux threshold instead of photon flux threshold. For simplicity, we have assumed photon index ~ 2 for all simulated sources. We convert the photon flux thresholds suggested by Gonthier et al. (2002) to energy flux threshold as $\sim 1.5 \times 10^{-10}$erg cm^{-2} s^{-1} for sources located in $|b| < 10°$ and $\sim 6.8 \times 10^{-11}$erg cm^{-2} s^{-1} for sources located in $|b| > 10°$ respectively.

5.2 Simulation results

We carry out Monte Carlo simulation of the Galactic pulsars born during the past 10 Myr. We find a total of 76 γ-ray mature pulsars of ages larger than 10^5 years old that could be detected by EGRET. Out of this simulated sam-

ple, 44 of them lie in the Galactic plane ($|b| \leq 5°$) and 32 lie in the higher latitude ($|b| > 5°$). This current result is slightly different from the simulations presented in Cheng et al. (2004a) because of the revised age restrictions here of taking only mature pulsars of $\geq 10^5$ years old. Currently, 4 radio pulsars with age $> 10^5$ yrs old are identified as γ-ray pulsars, i.e. Geminga, PSR B1055-52, PSR B1951+32, PSR J0218+42 (Thompson et al. 1996; Kuiper et al. 2000). The predicted γ-ray pulsar numbers appear very much larger than the confirmed γ-ray pulsars. We should notice that first not all 76 predicted are radio-loud. The radio beaming factor is roughly 0.15 (Emmering and & Chevalier 1989; Biggs 1990). Taking the radio beaming factor into account, we predict that $\sim$12 EGRET Unidentified Sources will be identified in radio band in future. In fact recently there are 20 known radio pulsars located within the error boxes of EGRET sources and many of them may be identified as radio-loud γ-ray pulsars (Manchester 2004). It is very important to note that TeV γ-rays from pulsar wind nebulae is isotropic and is independent of radio-loud or radio-quiet γ-ray pulsars.

In Figure 1, we plot the distributions of the pulsar period (upper panel) and the magnetic field (bottom panel) of our simulated sample, for both sources in the the high latitude of $|b| > 5°$ (solid histogram), and in the low latitude $|b| \leq 5°$ (dashed histogram). The proper motion velocity (top panel) and distance (bottom panel) distributions of our mature pulsar sample are presented in Figure 2. The average velocity of our sample is found to be ~ 350 km s^{-1}. We have taken this value in equation (5) to estimate the termination radius (cf. § 2.2). We show also in Figure 2 that the low and high latitude pulsar samples have different distance distributions. The average distance of the pulsars in the Galactic plane ($|b| \leq 5°$) is determined to be $< d > \simeq 900$ pc, while the average distance is $< d > \simeq 400$ pc for the high latitude sample ($|b| > 5°$). This suggests that many high latitude γ-ray mature pulsars may lie in the Gould Belt.

In Figure 3, we plot the γ-ray luminosity versus spin down power of our simulated γ-ray pulsar sample. The spin down power are found to be all lower than 10^{36} erg s^{-1}, which is consistent with our expectations. Many of them in the Galactic plane may be the Geminga-like pulsars. If we fit the simulated relation of γ-ray luminosity versus spin down power with single power law and it is consistent with the observed correlation of the known γ-ray pulsars, $L_{\gamma,\mathrm{GeV}} \propto L_{\mathrm{sd}}^{0.5}$ (Thompson 2001). However, from Figure 3 there probably exist two populations of the relations: one population follows $L_\gamma \propto L_{sd}$; another population emerges as a branch for $L_{sd} > 10^{34}$erg s^{-1}, with $L_\gamma \propto L_{sd}^{1/4}$. Zhang et al. (2004) have provided possible explanation for nature of these two populations and they estimate the separation of two populations should occur at $1.5 \times 10^{34} P^{1/3}$erg s^{-1}.

6 TEV SOURCE CANDIDATES OF THE UNIDENTIFIED EGRET SOURCES

Assuming that mature pulsars can form faint and compact nebulae, and can produce TeV photons through ICS processes, the ICS flux from the pulsar nebulae can be calculated by

$$F_{\gamma,\text{TeV}} = L^{\text{ICS}}/4\pi d^2 E_\gamma, \qquad (13)$$

where $L^{\text{ICS}} \simeq L_{\text{IC}} + L_{\text{SSC}}$ (see § 3), and E_γ is the threshold energy, taken to be 1 TeV. In order to calculate the TeV luminosity for each of simulated pulsars. we have to choose some fixed values for pulsar wind parameters, i.e. ϵ_e, ϵ_B, p and γ_w , which are produced in non-linear processes and will certainly vary from pulsar to pulsar. We have assumed a set of pulsar wind nebula parameters for all simulated pulsars, with $\epsilon_e \sim 0.5$ according to the energy equipartition assumption, $\epsilon_B \sim 0.01$, $p \sim 2.2$, $\gamma_w \sim 10^6$, and the ISM density $n \sim 1$ cm^{-3}. The choices of these parameters are consistent with the theoretical estimations.

In Figure 4, we plot the GeV γ-ray photon flux from the pulsar outer gap versus the TeV photon flux from the pulsar wind nebulae. There exists a correlation between the GeV and TeV fluxes because both quantities depend on the pulsar spin down power. This suggests that strong EGRET sources may be potential TeV sources to be detected by present and future TeV telescopes.

The TeV flux distribution of the mature pulsars in high latitude, $|b| > 5°$ (solid histogram) and on the Galactic plane, $|b| \le 5°$ (dashed histogram), are presented in Figure 5. The predicted TeV fluxes of the all our low latitude simulated sample are all lower than 3×10^{-12} photon cm^{-2} s^{-1}, which is also the upper flux limit all but two of the high latitude sample. The predicted TeV flux from our sample is lower than the previous observational constraints mentioned earlier in the Introduction. However, with the rapid advancements of the ground-based TeV telescopes, some of the unidentified EGRET sources could be identified as TeV sources in the future.

7   SUMMARY AND DISCUSSIONS

We study the high energy radiation from mature pulsars with the ages of $\sim 10^5 - 10^6$ years old in the present paper. We consider 100 MeV to GeV γ-rays generated from the magnetosphere of mature γ-ray pulsars based on a new self-consistent outer gap model, which includes the effects of inclination angle and the average properties of outer gap (Zhang et al. 2004). The relativistic wind particles from these mature pulsars interact with the interstellar medium, and form compact wind nebulae. The wind nebulae then produce X-ray emission through synchrotron radiation, and TeV photons from ICS by relativistic electrons on cosmic microwave background and synchrotron seed photons. We investigate the nebula radiation using a one-zone model, which has shown to be able to predict the high energy properties of known pulsar wind nebulae (Cheng et al. 2004b). We conclude that in mature pulsars, the synchrotron radiation and the ICS processes like SSC cannot significantly contribute in the 100 MeV to GeV energy band because of the weak magnetic field present ($B \sim 10^{-5}$ G). However, it is possible that the nebulae of young pulsars in the galactic plane surrounded by supernova remnants, e.g. the Crab nebula, can contribute to the 100 MeV to GeV energy band through synchrotron and SSC processes.

Finally, we calculate the TeV fluxes from wind nebulae of these mature pulsars through inverse Compton processes. The predicted TeV fluxes are consistent with the recent observational constraints obtained at the Whipple Observatory. In addition, our results predict that the unidentified EGRET sources, specially the strong sources, can be potential TeV sources to be be detected by future ground-based TeV telescopes. Several third generation ground-based TeV telescopes are recently finished or in construction, e.g., MAGIC (Lorenz 1999; 2004), HESS (Hofmann 1999; Hinton 2004), VERITAS (Weekes et al. 2002; Krennrich et al. 2004), and CANGAROO-III (Matsubara 1997; Kubo et al. 2004). The high sensitivity of these new TeV telescopes offer the possibility of investigating the unidentified EGRET sources. For example, **HESS is an imaging telescope array system with an array of four imaging atmospheric Cherenkov telescopes. Now it is fully operational, and its expected sensitivity at 1 TeV is about 2×10^{-13} photon cm^{-2} s^{-1}, then we also expect HESS could possibly detect TeV photons from about 15 unidentified EGRET sources if they are mature pulsars.**

REFERENCES

Aharonian, F. A. 1999, Astropart. Phys., 11, 225
Aharonian, F. A., Atoyan, A. M., & Kifune, T. 1997, A&A, 291, 162
Aharonian, F. A., et al. 1999, A&A, 346, 913
Aharonian, F. A., et al. 2000, ApJ, 539, 317
Aharonian, F. A., et al. 2002a, A&A, 390, 39
Aharonian, F. A., et al. 2002b, A&A, 393, L37
Aharonian, F. A., et al. 2005, A&A, 432, L9
Amenomori, M., et al. 1999, ApJ, 525, L93
Arons, J. & Scharlemann, E.T. 1979, ApJ, 231, 854
Arons, J. 1983, in Electron-Positron Pairs in Astrophysics, ed. M. L. Burns, A. K. Harding, & R. Ramaty (New York: AIP), 113
Atkins, R., et al. 2003, ApJ, 595, 803
Atoyan, A. M., & Aharonian, F. A. 1996, MNRAS, 278, 525
Bhattacharya, D., Wijers, R. A. M. J., Hartman, J. W., & Verbunt, F. 1992, A&A, 254, 198
Biggs, J. D. 1990, MNRAS, 245, 514
Bignami, G. F., & Caraveo, P. A. 1993, Nature, 361, 704
Caraveo, P. A., Bignami, G. F., DeLuca, A., Mereghetti, S., Pellizzoni, A., Mignani, R., Tur, A., & Becker, W. 2003, Science, 301, 1345
Chadwick, P. M., et al. 1998, Astropart. Phys., 9, 131
Cheng, A. F., & Ruderman, M. A. 1980, ApJ, 235, 576
Cheng, K. S., Ho, C., & Ruderman, M. A. 1986a, ApJ, 300, 500
Cheng, K. S., Ho, C., & Ruderman, M. A. 1986b, ApJ, 300, 521
Cheng, K.S., & Ding, K. Y. 1994, ApJ, 431, 724
Cheng, K. S., Ruderman, M. A., & Zhang, L. 2000, ApJ, 537, 964
Cheng, K. S., & Zhang, L. 1996, ApJ, 463, 271
Cheng, K. S., & Zhang, L. 1998, ApJ, 498, 327
Cheng, K. S., Zhang, L., Leung, P., & Jiang, Z.J. 2004a, ApJ, 608, 418
Cheng, K. S., Taam, R. E., & Wang, W. 2004b, ApJ, 617, 480
Chevalier, R. 2000, ApJ, 539, L45
Coroniti, F. V. 1990, ApJ, 349, 538
Daugherty, J. K., & Harding, A. K. 1996, ApJ, 458, 278
de Jager, O. C., & Harding, A. K. 1992, ApJ, 396, 161
Fan, G.L., Cheng, K.S. & Manchester, R.N. 2001, ApJ, 557, 297
Fegan, S.J. & Weekes, T.C. 2004, in Cosmic Gamma-Ray Sources, ed. K. S. Cheng & G. E. Romero, (Kluwer Academic Publishers), in press
Finley, J. P., Srinivasan, R., Saito, Y., Hiriyama, M., Kamae, T., Yoshida, K. 1998, ApJ, 493, 884

Gehrels, N., et al. 2000, Nature, 404, 363

Goldreich, P., & Julian, W.H. 1969, ApJ, 157, 859

Gonthier, P. L., Ouellette, M. S., Berrier, J., O'Brien, S., & Harding, A. K. 2002, ApJ, 565, 482

Grenier, I. A. 2000, A&A, 364, L93

Guillout, P. et al. 1998, A&A, 337, 113

Harding, A. K., & Zhang, B. 2001, ApJ, 548, L37

Hartman, R. C., et al. 1999, ApJS, 123, 79

Hester, J. J., et al. 1996, ApJ, 456, 225

Hinton, J.A. 2004, New Astronomy Reviews, 48, 331

Hofmann, W. 1999, in AIP Conf. Proc. 515, GeV-TeV Gamma Ray Astrophysics Workshop: Towards a Major Atmospheric Cherenkov Detector VI (New York: AIP), 500

Kennel, C. F., & Coroniti, F. V. 1984, ApJ, 283, 694

Kifune, T., et al. 1995, ApJ, 438, L91

Krennrich, F., et al. 2004, New Astronomy Reviews, 48, 345

Kuiper, L.W. et al. 2000, in Proceedings of Pulsar Astronomy - 2000 and beyond, IAU Colloquium, eds. M. Kramer, N. Wex and R. Wielebinski (San Francisco, ASP), 355

Kubo, H. et al. 48, New Astronomy Reviews, 48, 323

Lessard, R. W., et al. 2000, ApJ, 531, 942

Lorenz, E. 1999, in AIP Conf. Proc. 515, GeV-TeV Gamma Ray Astrophysics Workshop: Towards a Major Atmospheric Cherenkov Detector VI (New York: AIP), 510

Lorenz, E. 2004, New Astronomy Reviews, 48, 339

Lorimer, D. R., Bailes, M., & Harrison, P. A. 1997, MNRAS, 289, 592

Manchester, R. N. 2004, in Proceedings of Multiwavelengths Approach to Unidentified Gamma-ray Sources, eds. K.S.Cheng and G.E. Romero (ApSS)

Mathis, J. S., Metzger, P. G., & Panagia, N. 1983, A&A, 128, 212

Matsubara, Y. 1997, in Towards a Major Atmospheric Cherenkov Detector V, ed. O. C. de Jager (Potchefstroome University for CHE), 447

Moreno, E., Alfaro, E. J. & Franco, J. 1999, ApJ, 522, 276

Muslimov, A.G. & Harding, A.K. 2004, ApJ, 606, 1143

Olano, C.A. 1982, A&A, 112, 1950

Paczynski, B. 1990, ApJ, 348, 485

Pavlov, G. G., Zavlin, V. E., Sanwal, D., Burwitz, V., & Garmire, G. P. 2001, ApJ, 552, L129

Romani, R. 1996, ApJ, 470, 469

Ruderman, M. 1981, in IAU Sym. 95, Pulsars, ed. W. Sieber & R. Wielebinski (Dordrecht: Reidel), 87

Sari, R., Narayan, R., & Piran, T. 1996, ApJ, 473, 204

Sollerman, J., Lundqvist, P., Lindler, D., Chevalier, R. A., Fransson, C., Gull, T. R., Pun, C. S. J., Sonneborn, G. 2000, ApJ, 537, 861

Sturner, S. J., & Dermer, C. D. 1996, ApJ, 461, 872

Tanimori, T., et al. 1998, ApJ, 492, L33

Thompson, D. J. et al. 1996, ApJS, 107, 227

Thompson, D. J. 2001, in AIP Conf. Ser. 558, High Energy Gamma-Ray Astronomy, ed. F. A. Aharonian, & H. J. Völk (New York: AIP), 103

Weekes, T. C., et al. 1989, ApJ, 342, 379

Weekes, T. C., et al. 2002, Astropart. Phys., 17, 221

Weekes, T. C. 2004, in Cosmic Gamma-Ray Sources, ed. K. S. Cheng & G. E. Romero, (Kluwer Academic Publishers), 345

Willingale, R., Aschenbach, B., Griffiths, R. G., Sembay, S., Warwick, R. S., Becker, W., Abbey, A. F., & Bonnet-Bidaud, J.-M. 2001, A&A, 365, L212

Yoshikoshi, T., et al. 1997, ApJ, 487, L65

Zhang, L., & Cheng, K. S. 1997, ApJ, 487, 370

Zhang, L., & Cheng, K. S. 2003, A&A, 398, 639

Zhang, L., & Cheng, K. S. 2001, MNRAS, 320, 477

Zhang, L., Zhang, Y. J., & Cheng, K. S. 2000, A&A, 357, 957

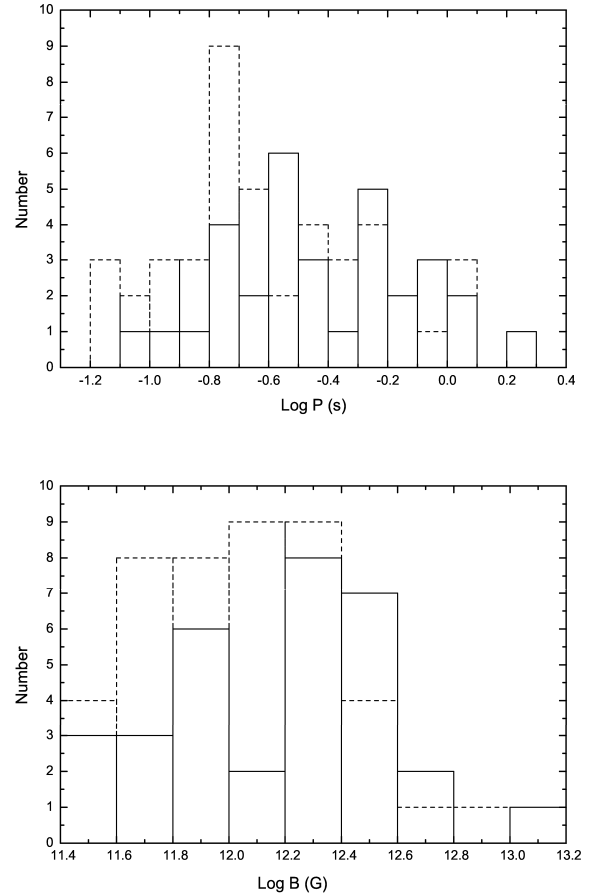Zhang, L., Cheng, K. S., Jiang, Z. J., & Leung, P. 2004, ApJ, 604, 317

Figure 1. The distribution of the period (upper panel) and surface magnetic field (bottom panel) of the simulated γ-ray pulsars which could be detected by EGRET. The distributions of the pulsars in the high latitude ($|b| > 5°$) (solid), and in the Galactic disk ($|b| \leq 5°$) (dashed) are shown.
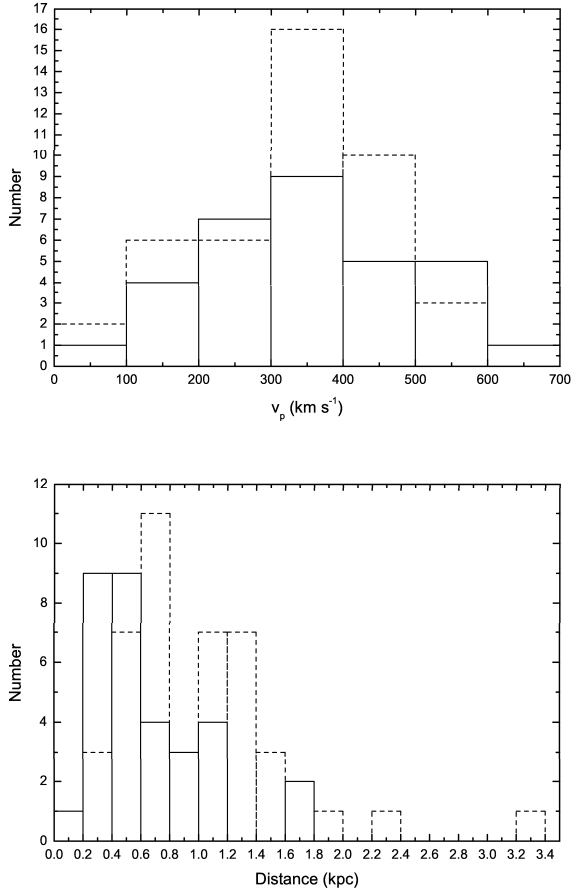
Figure 2. The distribution of the proper motion velocity (top) and the distance (bottom) of the simulated γ-ray pulsars. The distributions of the pulsars in the high latitude ($|b| > 5°$) (solid), and in the Galactic disk ($|b| \leq 5°$) (dashed) are shown.
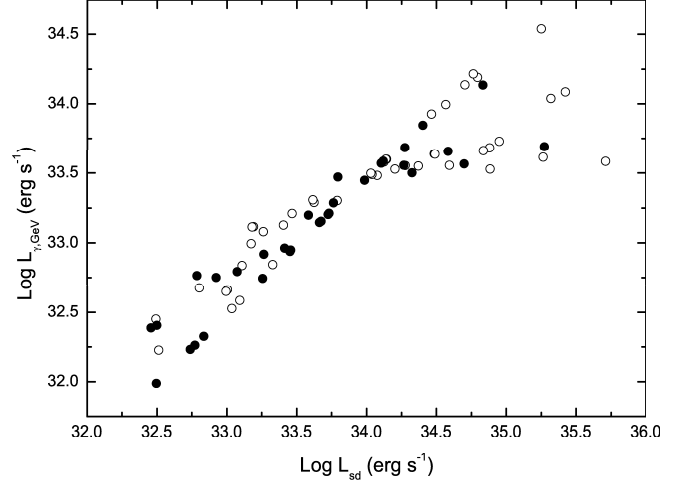

Figure 3. The GeV gamma-ray luminosity versus the spin down power for the simulated γ-ray pulsars for the high latitude $|b| > 5°$ (solid) and the Galactic latitude $|b| \leq 5°$ (circle) sample.

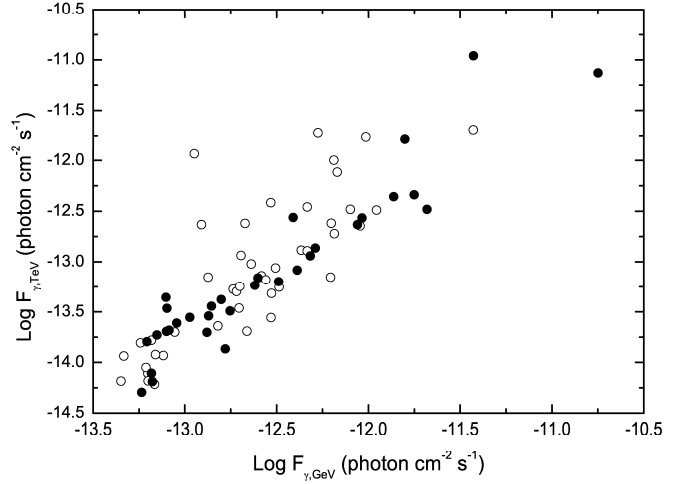**Figure 4.** The GeV gamma-ray flux versus the TeV flux for the simulated γ-ray pulsars for the high latitude $|b| > 5°$ (solid) and the Galactic latitude $|b| \leq 5°$ (circle) sample.
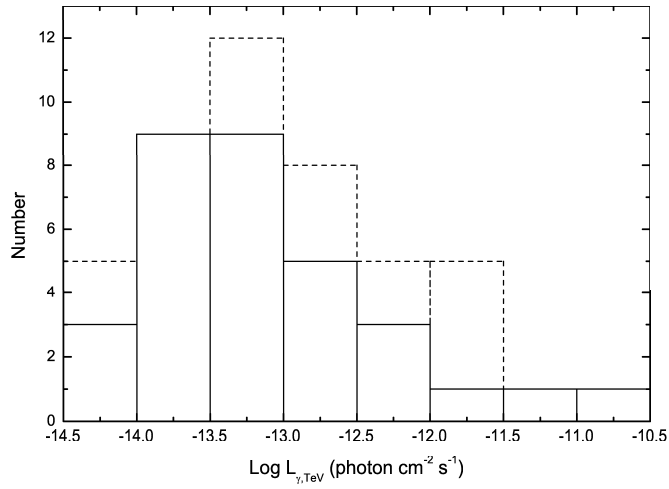
Figure 5. The distribution of the TeV flux from the wind nebulae of the simulated γ-ray pulsars which could be the unidentified EGRET sources. The distributions of the pulsars in the high latitude ($|b| > 5°$) (solid), and in the Galactic disk ($|b| \leq 5°$) (dashed) are shown.